# A single-shot transmissive spectrometer for hard x-ray free electron lasers

Diling Zhu, Marco Cammarata, Jan M. Feldkamp, David M. Fritz, Jerome B. Hastings, Sooheyong Lee, Henrik T. Lemke, Aymeric Robert, James L. Turner, and Yiping Feng

Citation: Appl. Phys. Lett. **101**, 034103 (2012); doi: 10.1063/1.4736725

View online: http://dx.doi.org/10.1063/1.4736725

View Table of Contents: http://aip.scitation.org/toc/apl/101/3

Published by the American Institute of Physics

# A single-shot transmissive spectrometer for hard x-ray free electron lasers

Diling Zhu,[a] Marco Cammarata,[b] Jan M. Feldkamp, David M. Fritz, Jerome B. Hastings, Sooheyong Lee,[c] Henrik T. Lemke, Aymeric Robert, James L. Turner, and Yiping Feng[a]
*Linac Coherent Light Source, SLAC National Accelerator Laboratory, 2575 Sand Hill Road, Menlo Park, California 94025, USA*

(Received 5 April 2012; accepted 25 June 2012; published online 16 July 2012)

We report hard x-ray single-shot spectral measurements of the Linac Coherent Light Source. The spectrometer is based on a 10 $\mu$m thick cylindrically bent Si single crystal operating in the symmetric Bragg geometry to provide dispersion and high transmission simultaneously. It covers a spectral range >1% using the Si(111) reflection. Using the Si(333) reflection, it reaches a resolving power of better than 42 000 and transmits >83% of the incident flux at 8.3 keV. The high resolution enabled the observation of individual spectral spikes characteristic of a self-amplified spontaneous emission x-ray free electron laser source. Potential applications of the device are discussed. © *2012 American Institute of Physics*. [http://dx.doi.org/10.1063/1.4736725]

The development of x-ray free-electron laser (FEL) sources[1–3] has and will continue to enable a broad range of scientific discoveries in many disciplines. Recent experiments at the Linac Coherent Light Source (LCLS) have explored light-matter interactions on the time and length scales of atoms,[4,5] demonstrated methods for structural determination of complex biological molecules and viruses,[6–8] and created high-energy-density states of matter commonly found in the interiors of large Jovian planets.[9] Current x-ray FEL sources operate on the principle of self-amplified spontaneous emission (SASE),[10,11] whose stochastic nature gives rise to shot-to-shot fluctuations in all beam properties, including pulse energy, duration, spatial profile, wavefront, temporal profile, and spectral content.[12] As FEL-based science areas develop, detailed knowledge of these properties becomes increasingly important for the interpretation of experimental data.

The quest to fully characterize these properties by single-shot, transmissive diagnostics with minimal perturbation has proven to be very challenging and has so far been demonstrated only for the case of pulse energy.[13,14] Methods of single-shot spectral characterization of the FEL source have been reported for hard[15] and soft[16] x-rays. However, both methods are destructive. In this Letter, we present the concept and experimental demonstration of a hard x-ray spectrometer capable of capturing the full SASE spectrum on a shot-by-shot basis whilst transmitting the majority of the pulse energy with minimal wavefront perturbation. When configured in the high-resolution geometry, individual SASE spectral spikes can also be resolved.

Ultrathin near-perfect silicon single-crystals were made available thanks to the rapid advancement in the semiconductor industry, and in particular, the silicon-on-insulator technology.[17] The spectrometer we report here utilized a 10 $\mu$m perfect crystal membrane (5 mm × 15 mm) of the shape of a diving board, which is bent to a radius of curvature between 100 and 300 mm. The small thickness allowed reaching bending curvatures previously inaccessible with thicker wafers and, at same time, provided high transmission for hard x-rays. Controlled bending was achieved by translating the free end of the membrane using a precision actuator. The dispersion geometry for the bent thin crystals is shown in Fig. 1. When an x-ray beam with a negligible divergence and finite bandwidth impinges onto the convex side of the curved crystal membrane, over the footprint of the x-ray beam on the crystal in the diffraction plane, different portions of the beam make different incident angles, each satisfying the Bragg condition for a slightly different wavelength $\lambda = 2d \sin\theta_B$ as given by Bragg's Law. $d$ is the lattice spacing for a given reflection and $\theta_B$ is the Bragg angle. Since for different wavelengths the reflection point walks on the

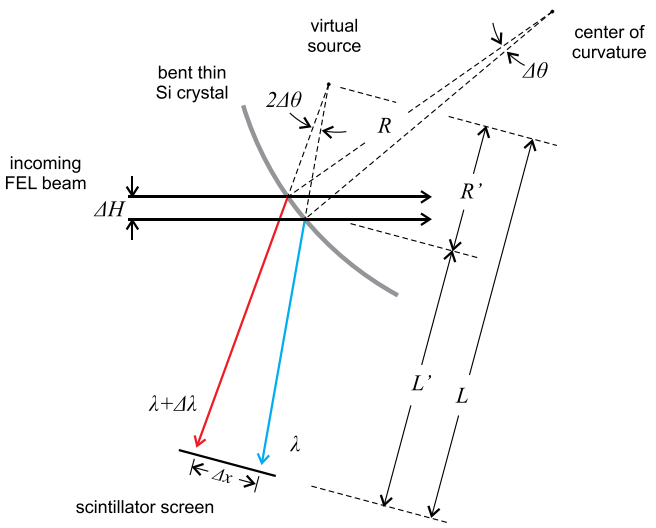


FIG. 1. Dispersion geometry of the spectrometer. The cylindrically bent crystal membrane diffracts dispersively a small percentage of the FEL beam to form the spectrograph, which is recorded on a scintillator-based detector positioned normal to the diffracted beam.

[a]Authors to whom correspondence should be addressed. Electronic addresses: dlzhu@slac.stanford.edu and yfeng@slac.stanford.edu.
[b]Current address: Institute of Physics, University of Rennes, 35042 Rennes, France.
[c]Current Address: Korea Research Institute of Standards and Science, 267 Gajeong-ro, Yuseong-gu, Daejeon 305-340, South Korea.

 

crystal surface, the reflected rays can be back-traced to a virtual source point located at a distance $R'$ from the crystal, where $R'$ is related to the crystal radius of curvature $R$ by the relation $R' = R\sin\theta_B/2$. Note that this configuration differs from well-known Bragg-type spectrometers with curved analyzers,[18–20] which are often optimized for spectroscopic studies where luminosity is of great importance. The dispersion $\Delta x$ on the detector plane for an energy increment of $\Delta E$ is given by

$$\Delta x = 2\tan\theta_B\left(\frac{R\sin\theta_B}{2} + L'\right)\frac{\Delta E}{E}, \quad (1)$$

where $L'$ is the distance from the membrane to the detector plane. The spectral range of the bent-crystal spectrometer depends on the footprint of the beam and $R$ as

$$\frac{\Delta E_{max}}{E} = \cot\theta_B\frac{H}{R\sin\theta_B}, \quad (2)$$

where $H$ is the beam size in the dispersion plane.

The experimental demonstration was performed at the x-ray pump probe (XPP) instrument at LCLS.[21] Two independent spectrometers were set up in tandem, as shown in Fig. 2(a), 192 m downstream from the end of the undulators. The FEL beam measured 400 $\mu$m FWHM with an angular divergence of 2 $\mu$rad FWHM in both the horizontal and the vertical direction at the spectrometer locations. The downstream spectrometer used the Si(111) reflection dispersing horizontally and covered the full range of the LCLS SASE pulse ($\sim$100 eV). The upstream spectrometer utilized the Si(333) reflection dispersing vertically, yielding a range of $\sim$20 eV but with a much higher resolution. The vertical dispersion geometry was chosen because of the direction of polarization of the x-ray FEL beam and the fact that the Bragg angle being close to 45° at 8.33 keV, the energy at which the experiment was performed. At this photon energy, the transmission of the spectrometers were 83% for Si(333) and 47% for Si(111). Thinner crystals can be used to further improve the transmission, but at the expense of broader Darwin curves which could impact resolution. The dispersed/reflected x-rays were then converted to visible light via a 100 $\mu$m thick Ce:YAG scintillator screen before being imaged and recorded by a high speed microscope.

A set of typical Si(111) spectra from 20 consecutive shots, operating at the nominal 150 pC bunch charge and optimal compression, is shown in Fig. 2(b). One selected spectrum is displayed in greater clarity in Fig. 2(c). These spectra are projections of the two-dimensional spectrographs normal to the dispersion direction. Each single shot spectrum appears distinctly different from the others and consists of a large number of spikes with varying width and magnitude. These shot-to-shot fluctuations in spectral content are characteristic of SASE as predicted by both theory[12] and simulations.[22] Their statistical characteristics are closely related to the temporal properties such as coherence time and pulse length, which are otherwise extremely difficult to measure. The wildly varying spectral signature of the SASE FEL pulses underscores the need for a single-shot diagnostic. The critical advantage of the high transmissivity of the current design is illustrated by the fact that the Si(111) spectrometer can be looked upon as the "experiment" whilst the upstream Si(333) spectrometer gives shot by shot spectral information. It is also important to note that the significantly increased resolution of the Si(333) spectrometer clearly shows details of unresolved features in the Si(111) spectra *albeit* over a smaller range, as shown in Fig. 2(d).

The dispersion relations of the two spectrometers were calibrated using a Si(111) channel-cut monochromator (CCM) to define the incoming wavelength. The monochromatized beam produced $\sim$1 eV wide line in the spectrograph normal to the dispersion direction. The lateral position of the lines are measured as a function of incoming photon energies and fitted to Eq. (1). For Si(111), the fit yielded $L = R' + L' = 365$ mm, which agrees well with the measured distance $L' = 330$ mm and $R'$ as derived from the radius of curvature of the crystal ($\approx$300 mm), calculated from the displacement at its free end. For Si(333), we doubled the amount of bending to provide a larger energy range. The fit

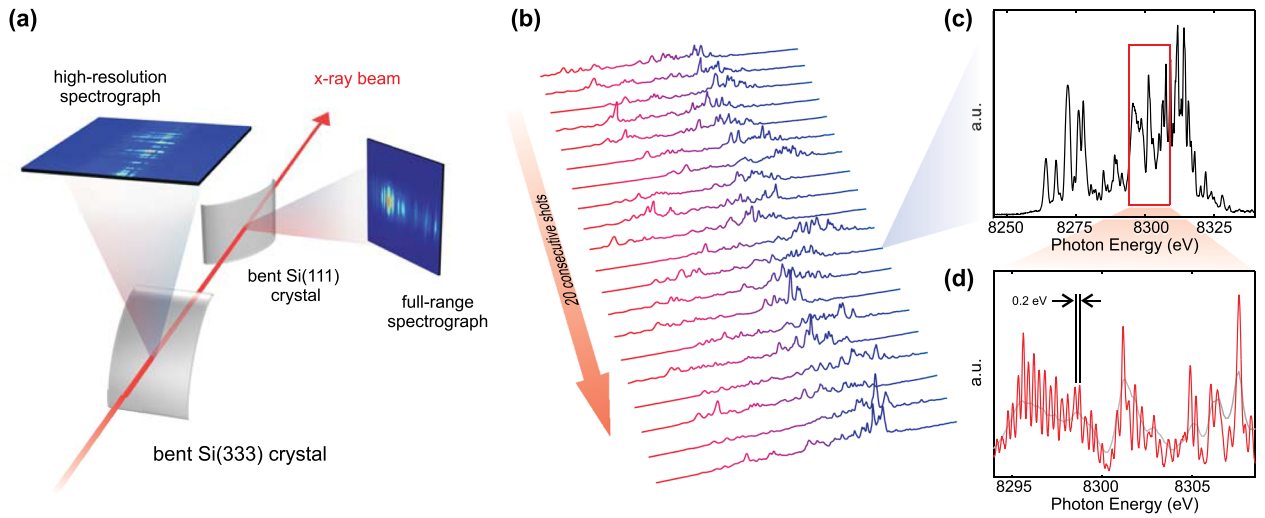


FIG. 2. (a) Schematics of the experimental setup. (b) Example of SASE spectra for 20 consecutive pulses recorded using the full-range Si(111) spectrometer. (c) The full-range Si(111) spectrum and (d) the high-resolution Si(333) spectrum of the same individual pulse (red) overlayed with the Si(111) measurement (gray).

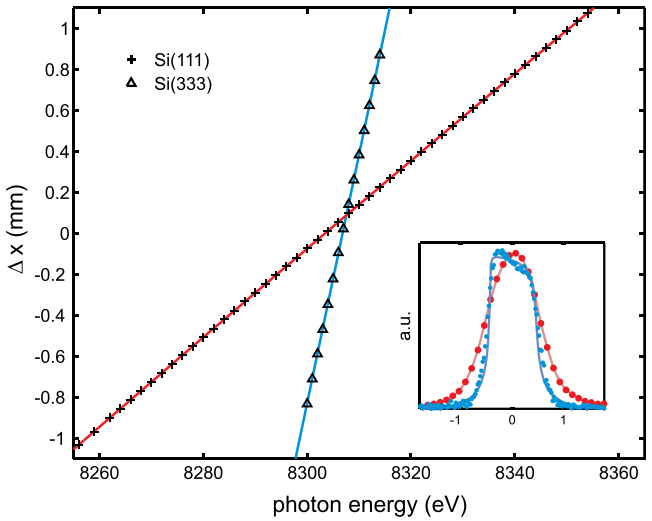


FIG. 3. Dispersion calibration of the spectrometer for both the Si(111) and Si(333) geometry. The red and blue curves are fitted lines using Eq. (1). The inset on the lower right shows the observed line shape with the red data points measured with the Si(111) spectrometer and blue data points Si(333). The red line is a Gaussian fit to the line shape measured by Si(111). The blue line is the theoretical line shape of the Si(111) rocking curve for comparison to the higher resolution Si(333) measurement, showing good agreement.

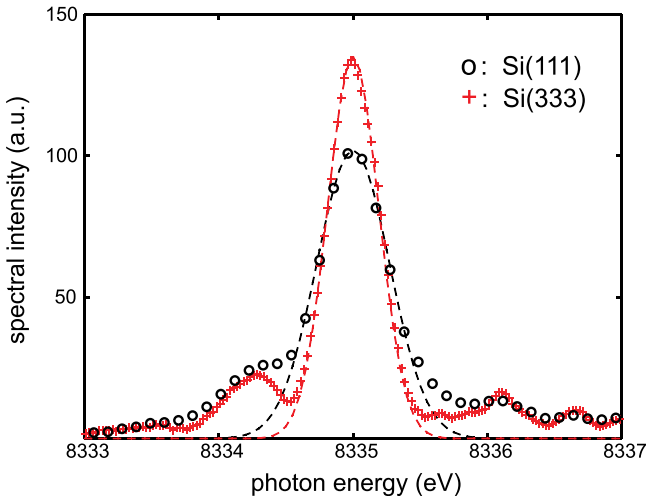


FIG. 4. Spectra of an individual FEL pulse reordered simultaneously by the Si(111) and Si(333) spectrometers while operating in the self-seeded mode. The red crosses are measurement obtained using the Si(333) spectrometer while the black circles are from the Si(111) spectrometer measurement. The dashed lines are Gaussian fits to the central peak, yielding FWHM values of 0.65 eV and 0.45 eV, respectively.

yielded $L = 495$ mm. With the measured $L' = 440$ mm, we obtain an estimated radius of curvature of $R = 150$ mm. The average intensity response of the spectrometer, i.e., the integrated reflectivity as a function of photon energy, was calibrated simultaneously with the dispersion relation using an intensity monitor upstream of the spectrometer setup. In the case of Si(111), a relatively flat response was observed as the FEL bandwidth lies well within the range of the spectrometer. However, for Si(333), the beam size became the limiting factor and the beam intensity profile modified the apparent spectral intensity. To obtain the correct spectrum, a normalization to the beam profile in the direction perpendicular to the dispersion is required (Fig. 3).

The diffraction-limited resolution function of the spectrometer is given by

$$\frac{\delta E}{E} = \cot(\theta_B)\frac{\delta x}{2(L'+R')}, \tag{3}$$

where $\delta x = \sqrt{(\delta x_s)^2 + (\delta x_e)^2 + (\delta x_d)^2}$ is the linear size of the spot formed by a perfectly monochromatic wave incident on the crystal. The spot size $\delta x$ includes three contributions: (1) the effective source size at the virtual point arising from a finite source divergence $\delta\Theta = 2\,\mu$rad contributes $\delta x_s = L\delta\Theta = 0.95\,\mu$m. (2) A finite extinction depth $\Lambda = 0.75\,\mu$m for Si(111) at 8.33 keV leading to a broadening of $\delta x_e \approx 2\Lambda\cot\theta_B = 6.2\,\mu$m. (3) The diffraction effect of the beam footprint of size $\delta R = 10.2\,\mu$m on the crystal surface where the diffracted beam is within the Darwin width $\omega_D = 34\,\mu$rad as calculated using the multilamellar theory[23–25] amounts to $\delta x_d \approx 1.39 \cdot \lambda L'/(\pi\delta R \sin\theta_B) = 11.9\,\mu$m. By combining these terms, we obtain $\delta x = 13.7\,\mu$m, or $\delta_{Si(111)} = 0.49$ eV as a lower bound. Other possible contributions from lattice strain and instrumental resolutions were found to be negligible. Using Eq. (3) for Si(333) yields $\delta_{Si(333)} = 0.1$ eV.

Experimentally, a direct estimate of the Si(111) spectrometer resolutions was determined to be $0.5 \pm 0.1$ eV by inspecting the apparent feature width and spacing in thousands of SASE spectra. A more careful characterization was derived from the line width measured when the FEL was operated in the self-seeded mode,[26,27] as shown in Fig. 4. The measured width is a convolution of the actual spectral width with that of the instrument resolution and can be written as $\delta E_{app} = \sqrt{\delta E_{act}^2 + \delta E_{instr}^2}$ (assuming each is of Gaussian line shape for simplicity). Based on the narrowest feature resolved with the Si(333) spectrometer, $\delta E_{instr,333} \lesssim 0.2$ eV. This indicates that the actual seeded spectrum width $\delta E_{act}$ is between the apparent width of 0.45 eV and the deconvoluted estimate $\sqrt{0.45^2 - 0.2^2} = 0.40$ eV. The resolution of the Si(111) spectrometer can in turn be estimated to be better than $\sqrt{0.65^2 - 0.40^2} = 0.51$ eV, and no worse than $\sqrt{0.65^2 - 0.45^2} = 0.47$ eV. This yields an estimate for the Si(111) spectrometer resolution of $0.49 \pm 0.02$ eV. It indicates that a significantly better resolution was achieved than the 1.19 eV given by the Si(111) Darwin width as a result of the dispersive geometry. For the Si(333) spectrometer, the resolution lower bound based on the finest features observed (cf. Fig. 2(d)) is in agreement with the 0.13 eV obtained from more sophisticated statistical analysis.[28] This allowed individual spectral spikes to be resolved for x-ray pulses of up to 25 fs in duration as, i.e., in the LCLS low-charge operating mode,[29] and would further enable pulse length and shape estimates from the Fourier relations connecting the spectral and temporal domains.

In summary, a transmissive single-shot hard x-ray spectrometer was conceived, built, and tested at LCLS, using ultra-thin cylindrically bent Si single crystals. Analysis of the experimental measurements indicates that the achieved spectral resolution and range are in good agreement with

theoretical estimates. The predicted SASE FEL spectrum was observed and shown to vary randomly in average wavelength and shape on a shot-to-shot basis. The use of the (333) reflection improved the spectral resolution to a level that revealed details down to the single-spike level.

The spectrometer presented here is already playing an important role in understanding and optimizing the FEL operating conditions at LCLS, revealing previously unseen spectral, spatial, and temporal characteristics. It will continue to enable FEL development activities such as the hard x-ray self-seeding[27] to proceed with real-time tuning and work towards achieving a transform-limited x-ray source with a peak power in the Terawatt regime.[22] More importantly, the additional spectral information is expected to benefit a broad range of scientific studies at FEL sources. Protein nanocrystallography, for example, currently copes with the spectral fluctuations of the FEL source by averaging tens of thousands of pulses.[6,8] The knowledge of the spectral content of each pulse may reduce the required data volume for structure determination significantly. Coherent diffractive imaging will also benefit from the additional spectral information, allowing more efficient uses of broadband x-ray sources.[26,30]

Y. Feng and D. Zhu are thankful to the staff of the Stanford Synchrotron Radiation Lightsource, especially B. Johnson and T. Hostetler for their continuing support to perform preliminary studies on the thin crystals. We would like to acknowledge helpful discussions with J. Krzywinski, A. Lutman, J. Arthur, Z. Huang, J. Wu, S.Moeller, M. Yabashi, P. Stefan, U. Bergmann, and R. Lee. We thank Y. Ning of Norcada for developing and supplying the thin crystals. Portions of this research were carried out at the Linac Coherent Light Source (LCLS) at the SLAC National Accelerator Laboratory. LCLS is an Office of Science User Facility operated for the U.S. Department of Energy Office of Science by Stanford University.

[1]P. Emma, R. Akre, J. Arthur, R. Bionta, C. Bostedt, J. Bozek, A. Brachmann, P. Bucksbaum, R. Coffee, F.-J. Decker *et al.*, Nat. Photonics **4**, 641 (2010).
[2]T. Ishikawa, Synchrotron Radiat. News **24**(4), 20 (2011).
[3]European XFEL facility in Hamburg, Germany. SwissFEL facility at the Paul Scherrer Institute in Switzerland. PAL-FEL in the Republic of Korea.
[4]L. Young, E. P. Kanter, B. Krässig, Y. Li, A. M. March, S. T. Pratt, R. Santra, S. H. Southworth, N. Rohringer, L. F. DiMauro *et al.*, Nature (London) **446**, 56 (2010).
[5]N. Rohringer, D. Ryan, R. A. London, M. Purvis, F. Albert, J. Dunn, J. D. Bozek, C. Bostedt, A. Graf, R. Hill *et al.*, Nature (London) **481**, 488 (2012).
[6]H. Chapman, P. Fromme, A. Barty, T. A. White, R. A. Kirian, A. Aquila, M. S. Hunter, J. Schulz, D. P. DePonte, U. Weierstall *et al.*, Nature (London) **470**, 73 (2011).
[7]M. M. Seibert, T. Ekeberg, F. R. N. C. Maia, M. Svenda, J. Andreasson, O. Jönsson, D. Odić, B. Iwan, A. Rocker, D. Westphal *et al.*, Nature (London) **470**, 78 (2011).
[8]A. Barty, C. Caleman, A. Aquila, N. Timneanu, L. Lomb, T. A. White, J. Addreasson, D. Arnlund, S. Bajt, T. R. M. Barends *et al.*, Nat. Photonics **6**, 35 (2011).
[9]S. Vinko, O. Ciricosta, B. I. Cho, K. Engelhorn, H. K. Chung, C. R. Brown, T. Burian, J. Chalupský, R. W. Falcone, C. Graves *et al.*, Nature (London) **482**, 59 (2012).
[10]A. M. Kondratenko and E. L. Saldin, Sov. Phys. Dokl. **24**, 986 (1979).
[11]R. Bonifacio, C. Pellegrini, and L. M. Narducci, Opt. Commun. **50**, 373 (1984).
[12]E. L. Saldin, E. A. Schneidmiller, and M. V. Yurkov, Nucl. Instrum. Methods A **407**, 291 (1998).
[13]Y. Feng, J. M. Feldkamp, D. M. Fritz, M. Cammarata, A. Robert, C. Caronna, H. T. Lemke, D. Zhu, S. Lee, S. Boutet *et al.*, Proc. SPIE **8140**, 81400Q (2011).
[14]S. P. Hau-Riege, R. M. Bionta, D. D. Ryutov, R. A. London, E. Ables, K. I. Kishiyama, S. Shen, M. A. McKernan, D. H. McMahon, M. Messerschmidt *et al.*, Phys. Rev. Lett. **105**, 043003 (2010).
[15]M. Yabashi, J. Hastings, M. S. Zolotorev, H. Mimura, H. Yumoto, S. Matsuyama, K. Yamauchi, and T. Ishikawa, Phys. Rev. Lett. **97**, 084802 (2006).
[16]P. Heimann, O. Krupin, W. F. Schlotter, J. Turner, J. Krzywinski, F. Sorgenfrei, M. Messerschmidt, D. Bernstein, J. Chalupsk, V. Hjkov *et al.*, Rev. Sci. Instrum. **82**, 093104 (2011).
[17]The thin crystal was fabricated by Norcada Inc. the surface roughness was measured to be below 2 nm r.m.s on both sides. A similar crystal but left un-bent had a rocking curve matching that of a perfect crystal as characterized at Beamline 2-2 of the Stanford Synchrotron Radiation Lightsource.
[18]H. H. Johann, Z. Phys. **69**, 185 (1931).
[19]T. Johansson, Z. Phys. **82**, 507 (1933).
[20]L. R. von Hamos, Ann. Phys. **17**, 716 (1933).
[21]XPP was one of the four hard x-ray instruments at LCLS. It was mainly designed to study ultrafast dynamics of matter at atomic scales driven by an optical laser.
[22]J. Wu, "Toward terrawatts one Angstrom free electron laser for LINAC Coherent Light Source upgrade," (unpublished).
[23]J. E. White, J. Appl. Phys. **21**, 855 (1950).
[24]G. Egert and H. Dachs, J. Appl. Crystallogr. **3**, 214 (1970).
[25]A. Boeuf, S. Lagomarsino, S. Mazkedian, S. Melone, P. Puliti, and F. Rustichelli, J. Appl. Crystallogr. **11**, 442 (1978).
[26]G. Geloni, V. Kocharyan, and E. Saldin, DESY Report No. 10-239, 2010.
[27]J. Amann, W. Berg, V. Blank, F.-J. Decker, Y. Ding, P. Emma, Y. Feng, J. Frisch, D. Fritz, J. Hastings *et al.*, "Demonstration of self-seeding in a hard x-ray free electron laser," Nat. Photonics (to be published).
[28]A. Lutman, J. Krzywinski, Z. Huang, Y. Feng, D. Zhu, D. M. Fritz, "Statistical analysis of the spectral properties of hard x-ray LCLS FEL," (unpublished).
[29]Y. Ding, A. Brachmann, F.-J. Decker, D. Dowell, P. Emma, J. Frisch, S. Gilevich, G. Hays, Ph. Hering, Z. Huang *et al.*, Phys. Rev. Lett. **102**, 254801 (2009).
[30]B. Abbey, L. W. Whitehead, H. M. Quiney, D. J. Vine, G. A. Cadenazzi, C. A. Henderson, K. A. Nugent, E. Balaur, C. T. Putkunz, A. G. Peele *et al.*, Nat. Photonics **5**, 420 (2011).